First-principles Study on Photocatalytic Properties of Cu_2O with Different Co Doped Concentrations

Qiaoya Lv[1], Yafang Li[1], Shuhua Shi[1], Junqing Zhao[1], Yanju Ji[1], Huilin Wang[1], Ting Chen[1], Yanjie Zhao[1], Liqiang Liu[2]and Luyan Li[1]*

[1]School of Science, Shandong Jianzhu University, Jinan 250101, China

[2]School of Materials Science and Engineering, Shandong Jianzhu University, Jinan 250101, China

*Corresponding author's e-mail: liluyan@sdjzu.edu.cn

Abstract. The electronic structure, photocatalytic properties and mechanism of Cu_2O with different Co-doped concentrations in visible light region are studied by first-principles calculation. The results show that intrinsic Cu_2O shows semiconductor characteristics, and the Co doped Cu_2O with 4.17% and 8.33% doping concentrations show metallic properties. The light absorption of Cu_2O in the visible region increases with the Co doping, and the photocatalytic efficiency enhances with increasing doping concentration. By analyzing the density of states, it is found that the enhanced light absorption of the two doped systems in the visible range is mainly caused by the intraband transition of Co 3d state electrons. The results found an effective way to improve the photocatalytic efficiency of Cu_2O in the visible region and promote the application of Cu_2O in photocatalysis.

1. Introduction

In recent years, the photocatalytic technology of inorganic semiconductor materials has shown broad application prospects in the fields of environmental management and energy conversion [1-5]. TiO_2 and ZnO are currently the most commonly used photocatalysts, while the band gap of TiO_2 and ZnO are between 3.0 and 3.4 eV, so they can only be stimulated by ultraviolet light (UV), which accounts for only 5% of sunlight [6]. The cubic Cu_2O is a metal-deficient P-type semiconductor with a band gap of 2.20 eV. It has many excellent features, such as strong adsorption capacity for oxygen, high absorption coefficient, non-toxicity, and low preparation cost, more importantly, the photocatalytic reaction of Cu_2O can be done under the visible light, which holds 45% of sunlight, so Cu_2O plays an important role in the photocatalysis, solar energy conversion, magnetic storage equipment, biosensing, anti-corrosion coatings and pesticide preparation [7-13].

Figure 1 shows the band position and band gap width of common semiconductor photocatalysts. It can be seen that the conduction band of Cu_2O is more positive than the energy capable of performing the reduction reaction, and the valence band is more negative than the energy of the photocatalytic oxidation reaction. Therefore, Cu_2O is a suitable catalyst for visible light reaction, but the photocatalytic efficiency of intrinsic Cu_2O in the visible light region is relatively low. In recent years, researchers have found that doping in semiconductor materials is an effective way to improve the photocatalytic efficiency. Vaiano et al. found that Pr doping can reduce the optical band gap of ZnO and ZnO displays photocatalytic activity in the visible region [14]; Jiang et al. confirmed that Au doping can improve the photocatalytic activity of Cu_2O in the visible region [15]; Zhang et al. found

that Zn doping can enhance the photocatalytic activity of Cu_2O in the visible region [16]; Peng et al. domonstrated that the band gap of Cu_2O decreases with the increase of Cl doping concentration, and the absorption capacity of Cu_2O for visible light is greatly improved [17]. However, there have few studies on Co-doped Cu_2O. In order to understand the influence of Co doping on Cu_2O, the electronic structure and optical properties of Co doped Cu_2O are calculated by first-principles calculation.

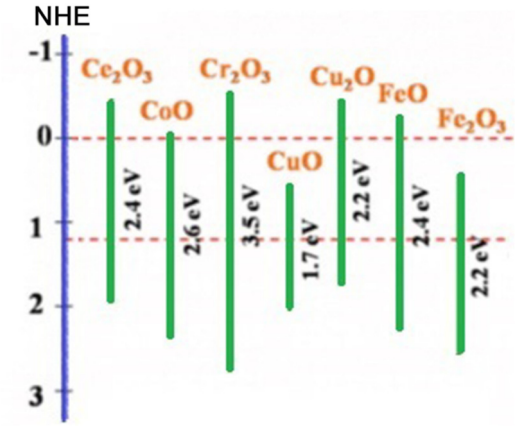

Figure 1 Band positions and bandgap widths of common semiconductor photocatalysts.

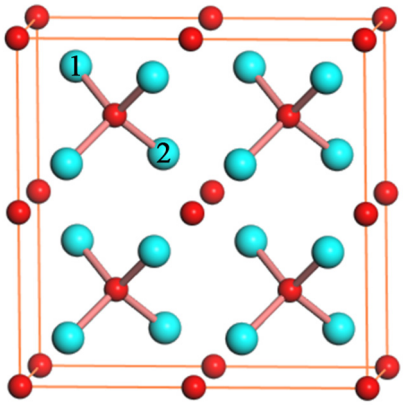

Figure 2 The supercell structure of 1×2×2 Cu_2O, red and blue are O and Cu atoms respectively, 1 and 2 are the positions of Co atoms

2. Calculation Method and Models

2.1. Calculation Method

The structure optimization and calculation of 1×2×2 Cu_2O supercell are carried out with Cambridge Serial Total Energy Package (CASTEP) based on density functional theory (DFT) and pseudopotential plane wave method[18,19]. The generalized gradient approximation (GGA) with Perdew-Burke-Ernzerhof (PBE) scheme is adopted for the exchange-correlation potential [20], the electron wave function is expanded in plane waves with a cutoff energy of 480 eV, ultrasoft pseudopotential and a monkhorst-pack grid with parameters of 4×2×2 is used for irreducible Brillouin zone sampling, the supercells are fully relaxed without any restriction using the Broyden-Fletcher-Goldfarb-Shanno (BFGS) method until the total energy of the system converges to 2×10^{-6} eV/atom and the force on each atom converges to less than 0.05 eV/Å [21]. After optimization with above parameters, the calculated lattice constant of the Cu_2O unit cell is 4.286 Å, which is almost the same as the experimental value (4.275 Å) [22]. Then the electronic structures and optical properties are calculated on the basis of the optimized supercells, and the numbers of k points are set as 6×3×3, the total energy of the system converges to 10^{-6} eV/atom.

2.2. Calculation Models

In order to clarify the photocatalytic properties and mechanism of Cu_2O in the visible region, the electronic structure and optical properties of pure and Co doped Cu_2O are calculated. As shown in figure 2, one Cu atom at position 1 is replaced with Co, which is written as Cu_2O-1Co with doping concentration of 4.17%; two Cu atoms at the positions 1 and 2 are replaced with Co atoms, written as Cu_2O-2Co with doping concentration of 8.33%.

3. Results and Discussion

3.1. Electronic structure analysis

The band structure of intrinsic Cu_2O is calculated firstly as shown in figure 3(a). It can be seen that the calculated Cu_2O is a direct band gap semiconductor with a band gap of 0.52 eV. Compared with the

experimental value of 2.20 eV, the calculated band gap is underestimated, which is attributed to the well-known intrinsic factor of DFT [23].

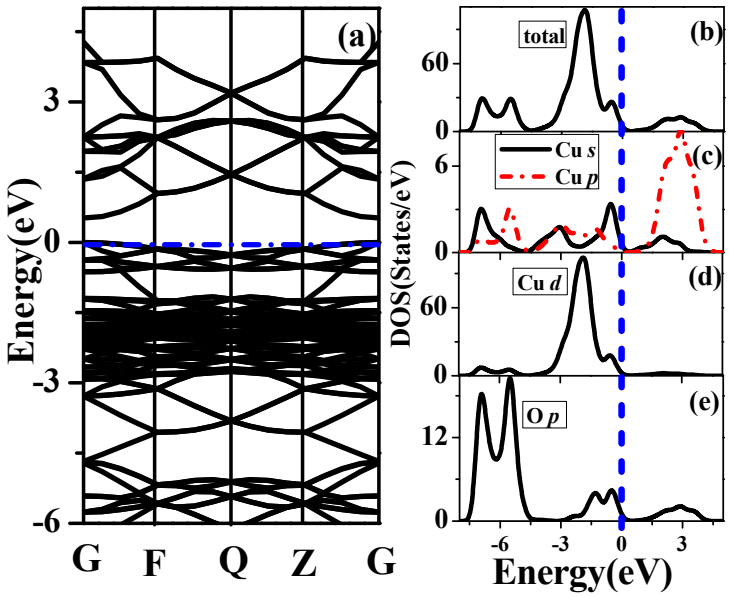

Figure 3 (a) Band structure, (b) the total density of states, (c)-(e) partial density of states of intrinsic Cu_2O.

Figure 3 (b-e) shows the density of states (DOS) and partial density of states (PDOS) of Cu_2O. It can be seen that the valence band can be divided into the lower valence band region and the upper valence band region. The lower valence band from -7.5 eV to -4.5 eV is derived from the O 2p states, and the upper valence band from -4.5 eV to 0 eV originates mainly from the Cu 3d states. In addition, the conduction band is dominated by Cu 3p and Cu 4s states. Electrons can transfer from the valence band to the conduction band, thus creating electron-hole pairs.

In order to compare the electronic structure with pure Cu_2O, the DOS and PDOS of Cu_2O-1Co and Cu_2O-2Co are studied respectively in figure 4. It can be seen that due to the doping of Co atoms, both the valence bands move upward and pass through the Fermi level, so the doping systems show metallic properties.

The valence band electronic states of Cu_2O-1Co pass through the Fermi level, then the electrons near the Fermi level can transfer from the occupied valence band to the non-occupied valence band, i.e. electrons can transfer with less energy than in the intrinsic Cu_2O, which will cause the absorption edge moves toward to low energy direction, and the optical band gap is red-shifted. This phenomenon can be seen more clearly in the absorption spectrum calculated below. In addition, it can be seen from figure 4(b-e) that, the states across the Fermi level are mainly contributed by the impurity state of Co 3d. The -1.5~0 eV energy range of Co 3d is occupied completely by electrons, and the 0~0.7eV energy range is empty state above the Fermi level.

For the Cu_2O-2Co system as shown in figure 4 (f-j), the DOS and PDOS are almost the same as that of Cu_2O-1Co, and the vicinity of the Fermi level is still mainly contributed by the impurity band of Co 3d state. However, it is worth noting that, the localization of Co 3d state in Cu_2O-2Co is weakened and the intensity is twice as high as the value of the Co 3d state in Cu_2O-1Co. Through the analysis above, for Cu_2O-2Co, more electron-hole pairs can generate by smaller energy, and the absorption edge will continue to move toward to low energy direction.

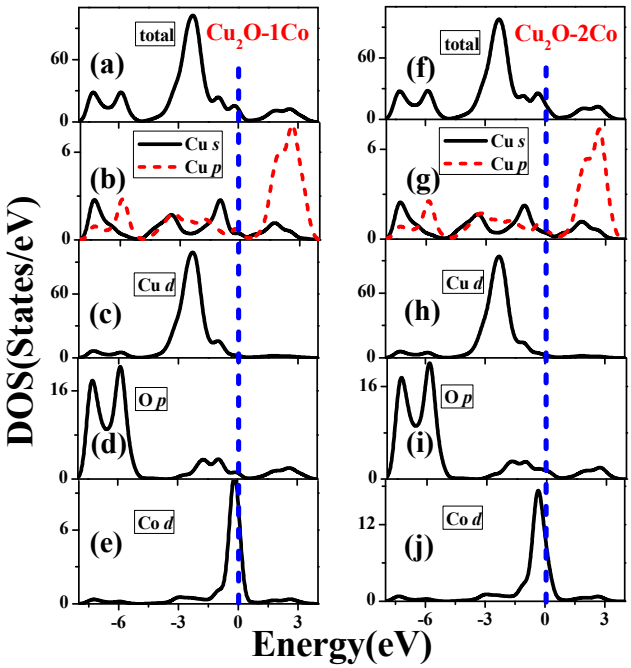

Figure 4 (a) Total density of states and (b)-(d) partial density of states of Cu_2O-1Co, (f) total density of states and (g)-(j) partial density of states of Cu_2O-2Co.

3.2. Optical property analysis

In order to analyze the optical properties of the systems, the imaginary part of dielectric function is analyzed firstly, figure 5 is the imaginary part of the dielectric function of the three systems. It can be seen from the figure that the intrinsic Cu_2O has weak electronic transition in the visible region, and there are two main peaks at 3.4 eV and 7.7 eV respectively. According to the analysis of DOS in figure 3, the peak at 3.4 eV may be due to the electronic transition from Cu 3d state to conduction band, the peak at 7.7 eV mainly caused by the electronic transition from O 2p state to Cu 3d state.

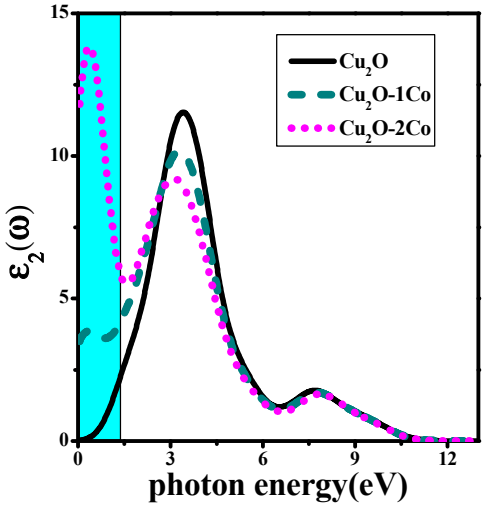

Figure 5 The imaginary part of the dielectric function for three structures, the blue area indicates the visible light energy range.

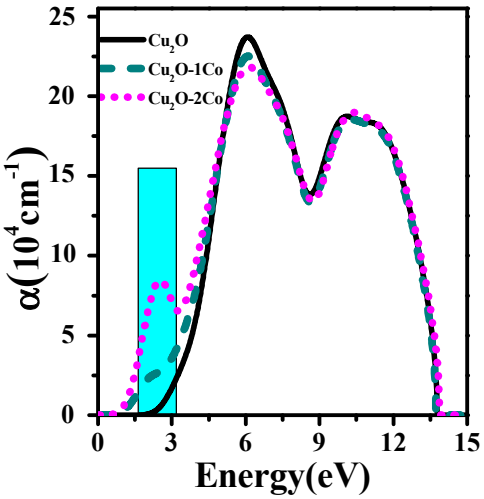

Figure 6 Absorption spectra of the three structures, the blue area indicates the visible light energy range.

Compared with Cu_2O, the amplitude values at the low energy region are significantly different for the doping systems. For Cu_2O-1Co system, a peak appears at 0.15 eV, and the amplitude values is significantly enhanced. By the analysis of figure 4, the Co 3d state passes through the Fermi level, so

the Co 3d electrons can transfer from the occupied state below the Fermi level to the non-occupied state above the Fermi level, the energy required for the intraband transition is smaller than the transition from valence band to conduction band of Cu_2O, so the electronic transition in the low energy range is mainly caused by the electronic intraband transition of the Co 3d state for Cu_2O-1Co.

Compared with Cu_2O-1Co system, noteworthy, the Cu_2O-2Co system has an extremely strong peak at the low energy region (near 0.30 eV). According to the analysis of the DOS and PDOS in figure 4, the Co 3d state of the Cu_2O-2Co is significantly stronger than that of Cu_2O-1Co, indicating that more electrons can participate intraband transition through small energy. The peak at 0.30 eV is also mainly caused by the intraband transition of Co 3d state electrons.

In order to further analyze the photocatalytic properties of the three systems, the absorption spectrum is calculated as shown in figure 6, the scissors approximation with the value of 1.68 eV is used for the calculated absorption edge to fit the experimental value [24]. It can be seen from figure 6 that the absorption ranges of the three systems are quite wide, and the main absorption part locates at the UV region, and the amplitudes in the UV region are almost the same, which indicates that doping has little effect in the short wavelength range.

Corresponding to the intensity of the imaginary part of the dielectric function in the visible light region, it also can be seen from figure 6 that, the intrinsic Cu_2O has little absorption, while the absorption peaks of Cu_2O-1Co and Cu_2O-2Co are enhanced with different degrees owing to the electronic intraband transition of the Co 3d state. With the increase of doping concentrations, the absorption intensity and the photocatalytic efficiency of Cu_2O are enhanced.

4. Conclusion

First-principle calculations have been performed to study the electronic structure and optical properties of intrinsic Cu_2O, Cu_2O-1Co and Cu_2O-2Co systems. The results show that the intrinsic Cu_2O is a direct band gap semiconductor with low absorption intensity in the visible region; both doping systems show metallic characteristics, and the light absorption in the visible region is stronger than that of the pure Cu_2O; as the Co doping concentration increases, the absorption intensity enhances in the visible region; different doping concentrations mainly affect the physical properties of Cu_2O in the long wavelength range, but have little effect in the short wavelength range. Based on the above studies, Co doping can improve the photocatalytic efficiency of Cu_2O in the visible region, which provides experimental reference and theoretical basis for the development of Cu_2O in photocatalysis.

Acknowledgement

This research was financially supported by the National Natural Science Foundation of China (21603122), Natural Science Foundation of Shandong Province of China (ZR2016FB03), and Doctoral Foundation of Shandong Jianzhu University (XNBS1266, XNBS1535, and XNBS1538).

References

[1] Su J, Lin Z, Chen G. (2016) Ultrasmall graphitic carbon nitride quantum dots decorated self-organized TiO_2 nanotube arrays with highly efficient photoelectrochemical activity. Appl. Catal., B., 186: 127-135.

[2] Li C, Chen G, Sun J, Rao J, Han Z, Hu Y, Xing W, Zhang C. (2016) Doping effect of phosphate in Bi_2WO_6, and universal improved photocatalytic activity for removing various pollutants in water. Appl. Catal., B, 188: 39-47.

[3] Lou S, Jia X, Wang Y, Zhou S. (2015) Template-assisted in-situ synthesis of porous AgBr/Ag composite microspheres as highly efficient visible-light photocatalyst. Appl. Catal. B., 176: 586-593.

[4] He Y R, Yan F F, Yu H Q, Yuan S J, Tong Z H, Sheng G P. (2014) Hydrogen production in a light-driven photoelectrochemical cell. Appl. Energy, 113: 164-168.

[5] Osterloh F E. (2013) Inorganic nanostructures for photoelectrochemical and photocatalytic water splitting. Chem. Soc. Rev, 42: 2294-2320.

[6] Gao X, LIU X X, Wang X J, Zhu Z M. (2016) Progress in Research on Modified Cu_2O Photocatalyst. J. Mater. Eng, 44: 120-128.
[7] Jiang D, Xue J, Wu L, Zhou W, Zhang Y, Li X. (2017) Photocatalytic performance enhancement of CuO/Cu_2O heterostructures for photodegradation of organic dyes: Effects of CuO morphology. Appl. Catal., B, 211: 199-204.
[8] Pang H, Gao F, Lu Q. (2010) Glycine-assisted double-solvothermal approach for various cuprous oxide structures with good catalytic activities. Crystengcomm, 12: 406-412.
[9] Das K, Sharma S N, Kumar M, De S K. (2010) Luminescence properties of the solvothermally synthesized blue light emitting Mn doped Cu_2O nanoparticles. J. Appl. Phys, 107: 433-147.
[10] Lu Y M, Chen C Y, Ming H L. (2005) Effect of hydrogen plasma treatment on the electrical properties of sputtered N-doped cuprous oxide films. Mater. Sci. Eng., B, 480: 482-485.
[11] Tang A D, Hu L Q, Wang D. (2011) Photo-catalytic property of Cu_2O prepared by room temperature liquid phase redox method. J. Funct Mater, 42: 2034-2037.
[12] Li L, Cheng Y, Wang W, Ren S, Yang Y, Luo X, Liu H. (2011) Effects of copper and oxygen vacancies on the ferromagnetism of Mn- and Co-doped Cu_2O. Solid State Commun, 151: 1583-1587.
[13] Zheng Z, Huang B, Wang Z, Guo M, Qin X, Zhang X, Wang P, Dai Y. (2009) Crystal Faces of Cu_2O and Their Stabilities in Photocatalytic Reaction. J. Phys. Chem. C, 113: 462-470.
[14] Vaiano V, Matarangolo M, Sacco O, Sannino D. (2017) Photocatalytic treatment of aqueous solutions at high dye concentration using praseodymium-doped ZnO catalysts. Appl. Catal., B, 209: 621-630.
[15] Jiang Z Q, Yao G, An X Y, Fu Y J, Gao L H, Wu W D, Wang X M. (2014) Electronic and optical properties of Au-doped Cu_2O: A first principles investigation. Chin. Phys. B, 23: 470-477.
[16] Zhang L, Jing D, Guo L, Yao X. (2014) In Situ Photochemical Synthesis of Zn-Doped Cu_2O Hollow Microcubes for High Efficient Photocatalytic H_2 Production. Acs Sustain Chem Eng, 2: 1446-1452.
[17] Peng J, Ren R K, Li J N, Zhang M J, Niu M, Ma L, Yan X B, Zhang S K. (2017) First Principles Calculation of Cl Doped Cu_2O. Micronanoelectronic Technology, 3: 157-161.
[18] Segall M D, Lindan P J D, Probert M J, Pickard C J, Hasnip P J, Clark S J, Payne M C. (2002) First-principles simulation: ideas, illustrations and the CASTEP code. J. Phys. Condens. Matter, 14: 2717-2744.
[19] Vanderbilt D. (1990) Soft self-consistent pseudopotentials in a generalized eigenvalue formalism. Phys. Rev. B, 41: 7892-7895.
[20] Perdew J P, Burke K, Ernzerhof M. (1996) Generalized Gradient Approximation Made Simple. Phys Rev Lett, 77: 3865-3868.
[21] Zhao R, Haskell W B, Tan V Y F. (2018) Stochastic L-BFGS: Improved Convergence Rates and Practical Acceleration Strategies. IEEE Trans. Signal Process, 66: 1155-1169.
[22] Katayama J, Ito K, Matsuoka M, Tamaki J. (2004) Performance of Cu_2O/ZnO Solar Cell Prepared By Two-Step Electrodeposition. J. Appl. Electrochem, 34: 687-692.
[23] Chen T, Pang J, He H, Peng Y, Wu N, Xu J, Du C X, Pang X X, Wu Z M, Cui Y T. (2017) Photoelectric properties of Mn-doped LiMgP new diluted magnetic semiconductor. Chin. Sci. Bull, 62: 4169-4178.
[24] Li L, Wang W, Liu H, Liu X, Song Q, Ren S. (2009) First Principles Calculations of Electronic Band Structure and Optical Properties of Cr-Doped ZnO. J. Phys. Chem. C, 113(19): 8460-8464.